ON-LINE APPENDIX

Radiomic Feature Description

We evaluated 326 imaging radiomics features, which are divided into 3 sets as follows:

Set 1: First-Order Statistics

First-order statistics (34 features) describe the distribution of voxel intensities within the CT/CTA image. The selected measures were the following: mean, SD, median, minimum, maximum, entropy, mode, energy, the first 7 standardized moments around the mean, a normalized histogram of 20 bins ranging from 0 to 200 for NCCT and 20 bins ranging from 0 to 500 for CTA images, and the histogram bin with the highest count, skewness, and kurtosis.[1]

Set 2: Shape and Size-Based Features

In the set 2 group of features, we included descriptors of the 3D size and shape of the thrombus region. The measures used (6 features) included compactness, surface area, thrombus length, volume size, and surface-to-volume ratio.[2]

Set 3: Textural Features

Gray-Level Co-Occurrence Matrix. Gray-level co-occurrence matrix (GLCM) ($n = 78$), also known as the gray-level spatial dependence matrix, characterizes the texture of an image by calculating how often pairs of pixels with specific values and in a specified spatial relationship occur in an image, creating a GLCM, and then extracting statistical measures from this matrix. In this article, co-occurrences with a distance of 1 pixel were calculated in horizontal, vertical, and diagonal orientations ($\theta = 0, 45, 90, 135$) for intensity bins with widths 5 HU for NCCT and 10 for CTA images. For the axial, coronal, and sagittal planes, 1 co-occurrence matrix was constructed including all slices, and the mean and SD of the 4 orientations were calculated per plane for 13 measures, such as autocorrelation, contrast, correlation, cluster prominence, dissimilarity, energy, entropy, homogeneity, maximum probability, sum average, sum entropy, and 2 information measures of correlation.[3]

Gray-Level Run Length. Rather than looking at pairs of pixels, the gray-level run length ($n = 66$) looks at runs of pixels—that is, how many pixels of a given gray value occur in a sequence in a given direction.[4] In this article, runs with $\theta = 0$, 45, 90, and 135 were calculated in the axial, coronal, and sagittal views. Measures such as short run emphasis, long run emphasis, gray-level nonuniformity, run length nonuniformity, run percentage, low gray-level run emphasis, high gray-level run emphasis, short run low gray-level emphasis, short run high gray-level emphasis, long run low gray-level emphasis, and long run high gray-level emphasis were calculated and averaged over the 4 orientations for each plane. All measures were calculated for both intensity bins of width 5 HU for NCCT and width 20 HU for CTA images.[2,5]

Neighborhood Gray-Tone Difference Matrix. The neighborhood gray-tone difference matrices ($n = 10$) are based on the differences between each voxel and the neighboring voxels in the adjacent image planes.[6] Texture parameters derived from the neighborhood gray-tone difference matrix resemble the human perception of the image. Five measures of coarseness, contrast, busyness, complexity, and strength were calculated. We calculated the mean difference with the surrounding voxels in a 3D 26 neighborhood for intensity bins of 1 and 10. The 5 measures were calculated for both of these settings and both image modalities.

Laws Texture. Laws measures texture energy ($n = 105$) by convolution of the image with 1D kernels.[7] We used five 1D kernels: 1, 4, 6, 4, 1 (level, L); −1, −2, 0, 2, 1 (edge, E); −1, 0, 2, 0, −1 (spot, S); 1, −4, 6, −4, 1 (ripple, R); and −1, 2, 0, −2, 1 (wave, W), which created 125 3D kernels: LLL, LLE, and so forth. After convolution, the mean, absolute mean, and SD over the ROI and averaged measures of rotated kernels were calculated, resulting in 35 kernels with 3 measures each.

Local Binary Pattern. Local binary pattern ($n = 27$) is a type of visual descriptor for classification in computer vision. Local binary pattern is the particular case of the texture spectrum model[8,9] and a powerful feature for texture classification. Local binary pattern measures the homogeneity of texture by determining the number of transitions from intensities higher than each central pixel to intensities lower than that central pixel. In this study, the number of "regions" higher or lower in intensity around each voxel in a 26 and a 98 neighborhood were applied. The mean and SD of the number of regions were calculated.

REFERENCES

1. Awad J, Krasinski A, Parraga G, et al. **Texture analysis of carotid artery atherosclerosis from three-dimensional ultrasound images.** *Med Phys* 2010;37:1382–91 CrossRef Medline
2. Aerts HJ, Velazquez ER, Leijenaar RT, et al. **Decoding tumour phenotype by noninvasive imaging using a quantitative radiomics approach.** *Nat Commun* 2014;5:4006 CrossRef Medline
3. Soh LK, Tsatsoulis C. **Texture analysis of SAR sea ice imagery using gray level co-occurrence matrices.** *IEEE Trans Geosci Remote Sens* 1999;37:780–95 CrossRef
4. Galloway MM. **Texture analysis using gray level run lengths.** *Computer Graphics and Image Processing* 1975;4:172–79 CrossRef
5. Tang X. **Texture information in run-length matrices.** *IEEE Trans Image Process* 1998;7:1602–09 CrossRef Medline
6. Amadasun M, King R. **Textural features corresponding to textural properties.** *IEEE Transactions on Systems, Man, and Cybernetics* 1989; 19:1264–74 CrossRef
7. Laws KI. **Rapid texture identification.** In: Weiner TF. *Image Processing for Missile Guidance.* Bellingham: Society of Photo-optical Instrumentation Engineers; 1980
8. Wang L, He DC. **Texture classification using texture spectrum.** *Pattern Recognition* 1990;23:905–10 CrossRef
9. Topi M, Timo O, Matti P, et al. **Robust texture classification by subsets of local binary patterns.** In: *Proceedings 15th International Conference on Pattern Recognition*, Barcelona, Spain. September 3–7, 2000; 708–71

On-line Table 1: Baseline characteristics of patients included in the study stratified by recanalization status

Variable	Recanalization with IV Alteplase (n = 30)	No-Recanalization with IV Alteplase (n = 37)	P Value
Clinical			
Age (median) (IQR) (yr)	75 (68–81)	77 (69–83)	.30
Sex (male) (No.) (%)	13 (43%)	17 (46%)	.45
Baseline NIHSS (median) (IQR)	14 (12–19)	16 (10–20)	.37
History of coronary artery disease (No.) (%)	4 (13.3%)	4 (10.8%)	.25
History of stroke/TIA (No.) (%)	8 (26.7%)	4 (10.8%)	.02
History of hypertension (No.) (%)	18 (60.0%)	18 (48.6%)	.16
History of dyslipidemia (No.) (%)	10 (33.3%)	12 (32.4%)	>.99
History of antiplatelet use (No.) (%)	10 (33.3%)	9 (24.3%)	.22
History of atrial fibrillation (No.) (%)	8 (26.7%)	9 (24.3%)	.81
Anticoagulation (No.) (%)	4 (13.3%)	2 (5.4%)	.15
History of diabetes (No.) (%)	6 (20.0%)	4 (10.8%)	.07
History of smoking (No.) (%)	14 (46.7%)	9 (24.3%)	.06
Heart rate (median) (IQR) (per min)	77 (66–91)	74 (66–88)	.75
Systolic blood pressure (median) (IQR) (mm Hg)	143 (124–156)	140 (128–150)	.17
Diastolic blood pressure (median) (IQR) (mm Hg)	79 (65–86)	77 (66–86)	.55
Blood glucose level (median) (IQR) (mmol/L[a])	6.7 (6.1–8.0)	7.1 (6.1–7.9)	.93
Serum creatinine level (median) (IQR) (mmol/L[a])	73.8 (65.2–91.1)	85.3 (61.0–100.2)	.27
Hematocrit level (%) (median) (IQR)	0.4 (0.38–0.43)	0.42 (0.38–0.45)	>.99
Platelet count (median) (IQR) 10^9/L	208 (158–259)	219 (189–261)	.23
International normalized ratio (median) (IQR)	1.0 (1–1.2)	1.0 (1–1.1)	.99
PTT (median) (IQR) (sec)	29.8 (27.1–31.5)	28.1 (26.7–30.6)	.85
Total cholesterol level (mmol/L[a]) (median) (IQR)	4.7 (3.9–5.6)	5.1 (4.4–7.3)	.37
Etiology of ischemic stroke			
Extracranial large-artery disease (No.) (%)	2 (6.7%)	6 (16.2%)	.50
Intracranial artery disease (No.) (%)	2 (6.7%)	1 (2.7%)	
Cardioembolic (No.) (%)	14 (46.7%)	19 (51.4)	
Other causes (No.) (%)	0	1 (2.7%)	
Undetermined (No.) (%)	2 (6.7%)	10 (33.3%)	
Imaging			
Baseline ASPECTS on NCCT (median) (IQR)	8 (7–10)	8 (6–9)	.43
ICA occlusion (No.) (%)	1 (3.3%)	10 (27.0%)	<.01
Proximal M1 segment MCA occlusion (No.) (%)	6 (20%)	12 (32.4%)	.02
Distal M1 segment MCA occlusion (No.) (%)	23 (76.7%)	20 (54.1%)	.12
Onset-to-CT imaging time (median) (IQR) (min)	119 (85–171)	123 (90–174)	.15
CT imaging-to-recanalization assessment time (median) (IQR) (min)	225 (126–283)	130 (60–210)	<.01
IV alteplase-to-recanalization assessment time (median) (IQR)	204 (94–274)	101 (35–196)	<.01

Note:—IQR indicates interquartile range; PTT, partial thromboplastin time.

On-line Table 2: The best selected radiomics features from each group[a]

Feature Set	Feature Name
NCCT features ($n = 5$)	SD of maximum probability of gray-level co-occurrence matrix with the level number of 60 at axial orientation
	Skewness
	Mean of Laws LSW
	SD of Laws spot-ripple waves
	SD of Laws spot-spot ripple
CTA features ($n = 15$)	Proportion of pixel numbers with 110–135 HU to the total number of clot pixels
	Homogeneity of GLCM with the level number of 60 at coronal orientation
	Short run emphasis of GLRLM with the level of 30 at coronal orientation
	Proportion of pixel numbers with 110–135 HU to the total number of clot pixels
	Short run emphasis of GLRLM with the level of 30 at sagittal orientation
	Proportion of pixel numbers with 0–25 HU to the total number of clot pixels
	Short run emphasis of GLRLM with the level of 30 at sagittal orientation
	Mean of Laws level-ripple waves
	Homogeneity of GLCM with the level number of 60 at sagittal orientation
	Nonuniformity of run length of 120 of GLRLM at coronal orientation
	Homogeneity of GLCM with the level number of 60 at axial orientation
	Run percentage of GLRLM with the level of 30 at axial orientation
	Mean of Laws ripple-ripple ripple
	Short run gray-level emphasis of GLRLM with the level of 30 at coronal orientation
	Run percentage of GLRLM with the level of 120 at axial orientation
	Mean of Laws level-spot ripple
Radiomics change features ($n = 6$)	Proportion of pixel numbers with 110–135 HU to the total number of clot pixels
	Mean Laws LSW
	Homogeneity of GLCM with the level number of 60 at coronal orientation
	Energy of GLCM with the level number of 60 at sagittal orientation
	Absolute mean of Laws LSS
	Absolute mean of Laws LLS
Combined features ($n = 12$)	Proportion of pixel numbers with 110–135 HU to the total number of clot pixels in radiomics change group
	Proportion of pixel numbers with 110–135 HU to the total number of clot pixels in CTA feature group
	Mean of Laws LSW in radiomics change group
	SD of maximum probability of GLCM with the level number of 60 at axial orientation in NCCT feature group
	Skewness in NCCT feature group
	Homogeneity of GLCM with the level number of 60 at coronal orientation in radiomics change group
	Homogeneity of GLCM with the level number of 60 at coronal orientation in CTA feature group
	Energy of GLCM with the level number of 60 at sagittal orientation in radiomics change group
	Absolute mean of Laws LSS in radiomics change group
	Absolute mean of Laws LLS in CTA feature group
	Short run emphasis of GLRLM with the level of 30 at coronal orientation in CTA feature group
	SD of Laws SSW in NCCT feature group

Note:—GLRLM indicates gray-level run length matrix; LSS, level-spot spot; LLS, level-level spot; SSW, spot-spot-wave.
[a] The numbers in parentheses are the number of the selected features for each group.

On-line Table 3: Parameter settings for the used support vector machine classifier in Matlab[a]

Parameters	Learner	λ	K-Fold	Fitted Loss	Regularization	Others
Values	Svm	0.02	5	Hinge	Ridge (L2)	Default

[a] From fitclinear (https://www.mathworks.com/help/stats/fitclinear.html).

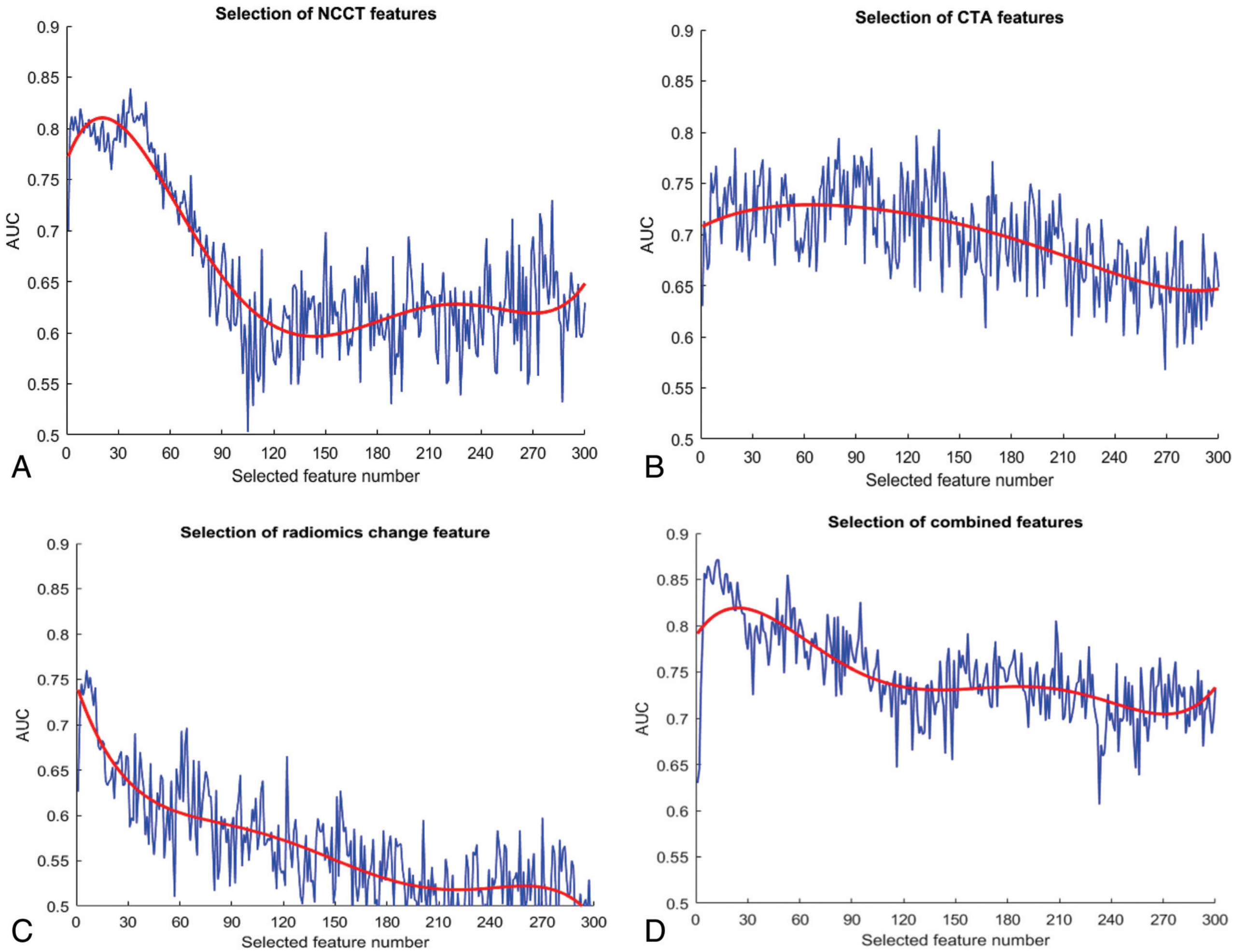

ON-LINE FIG 1. Determination of the optimal number of selected features.

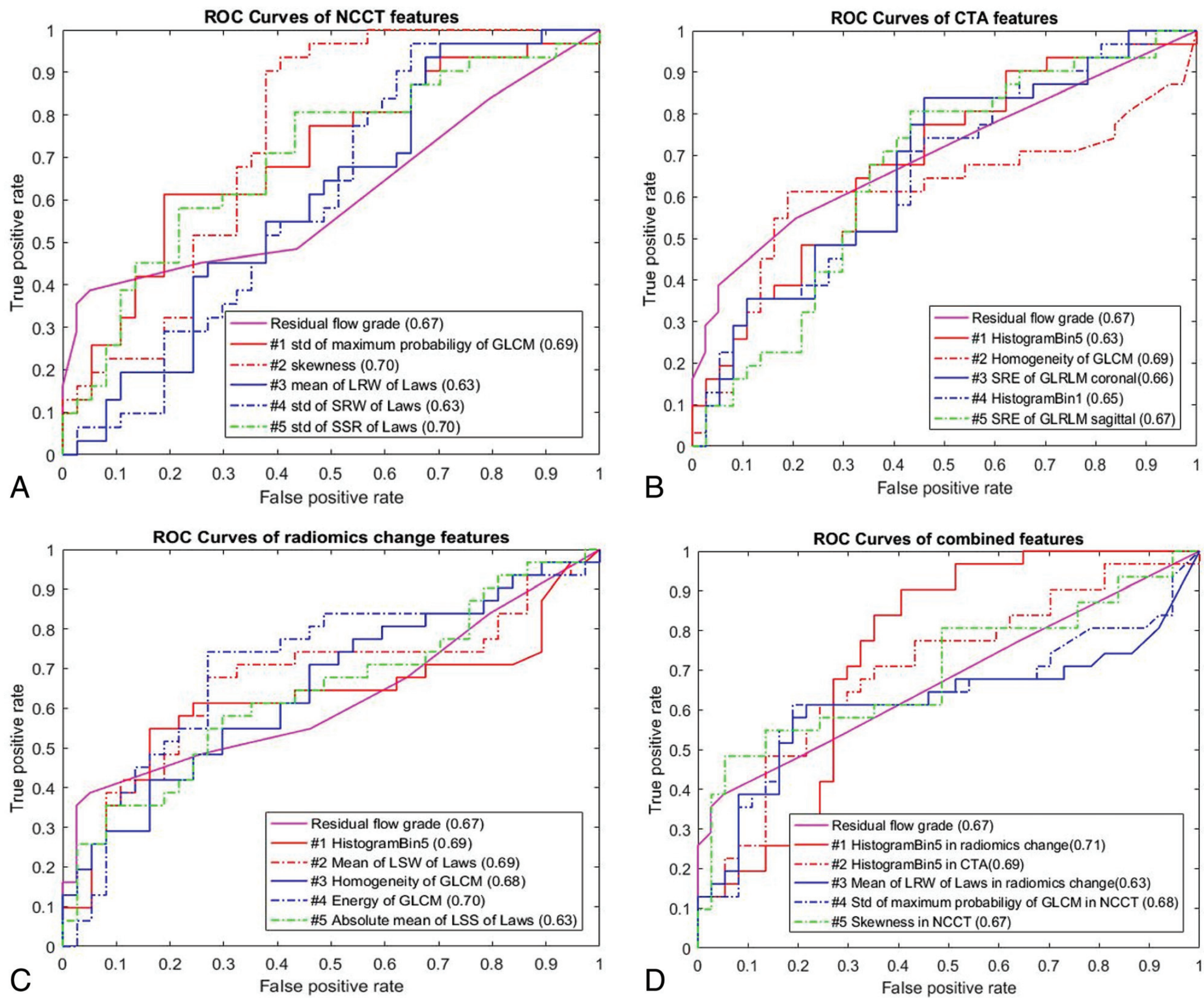

ON-LINE FIG 2. ROC curves of different features from different feature groups compared with nonradiomics feature of residual flow grade.